SLAC-PUB-10908
June 2005

Hybrid FDTD Analysis for Periodic On-Chip Terahertz (THz) Structures

Yasser A. Hussein* and James E. Spencer
Stanford Linear Accelerator Center-Stanford University, Menlo Park, CA USA
yasser@slac.stanford.edu, jus@slac.stanford.edu

Abstract- We present electromagnetic analysis and radiation efficiency calculations for on-chip terahertz (THz) structures based on a hybrid, finite-difference, time-domain (HFDTD) technique. The method employs the FDTD technique to calculate S-parameters for one cell of a periodic structure. The transmission ABCD matrix is then estimated and multiplied by itself *n* times to obtain the *n*-cell periodic structure ABCD parameters that are then converted back to S-parameters. Validation of the method is carried out by comparing the results of the hybrid technique with FDTD calculations of the entire periodic structure as well as with HFSS which all agree quite well. This procedure reduces the CPU-time and allows efficient design and optimization of periodic THz radiation sources. Future research will involve coupling of Maxwell's equations with a more detailed, physics-based transport model for higher-order effects.

I. Introduction

Recently, we explored possibilities for producing narrow-band THz radiation using either free or bound electrons (solid state) in micro-undulatory periodic configurations [1] because integrated circuit technology appeared well matched to this region extending from about 300 GHz to 30 THz. This range has largely been neglected until recently because it runs from the limit of WR-3 waveguide around 300 GHz up to CO_2 lasers where the laser regime becomes dominant. An excellent review of terahertz technology and its applications in biology and medicine can be found in the papers by Siegel [2]-[3]. There are two basic approaches for generating THz radiation - free and bound electron (BE) implementations. Herein, the emphasis is on producing radiation using bound electrons via IC technology as opposed to, e.g., free electron lasers (FELs) that are bulky, expensive, need high power and have low efficiencies [4]. While accurate modeling of the proposed implementation requires coupling of Maxwell's equations with an appropriate, physics-based transport model, we concentrate on the electromagnetic analysis based on the assumption of ballistic transport and that radiative losses are much greater than for other loss mechanisms, i.e. conductor, thermal or substrate losses.

II. General Discussion and Analogy

The most direct approach to obtain the radiation pattern is to determine the Poynting vector based on calculating the acceleration fields in the far field and from them the angular distribution:

$$\frac{dP}{d\Omega} = \frac{1}{4\pi c^3}\left\{\boldsymbol{n} \times \int \frac{\partial \boldsymbol{J}(\boldsymbol{r}', t_r)}{\partial t} d\boldsymbol{r}'\right\}^2 \qquad (1)$$

where t_r is the retarded time between source and detector, $\boldsymbol{J}$ is the current density, P is the

Contributed to 2005 IEEE/ACES International Conference on Wireless Communications and Applied Computational Electromagnetics, April 3-7, 2005, Honolulu, HI, USA

Work supported by Department of Energy contract DE-AC02-76SF00515

power, and c is the speed of light. For $\beta \equiv \boldsymbol{\upsilon}/c \ll 1$, the above relation reduces to the Larmor relations:

$$\frac{dP}{d\Omega} = \frac{e^2}{4\pi c^3}\left\{\frac{d\upsilon(t)}{dt}\right\}^2 \sin^2\theta \quad \text{and} \quad P = \frac{2}{3}\frac{e^2}{c^3}\left\{\frac{d\upsilon(t)}{dt}\right\}^2 \qquad (2)$$

where θ is the angle between the observation direction $\boldsymbol{n}$ and the direction of acceleration at emission time t. A straightforward application of Eq. (1) was given in Eq. (1) of Ref. [1] where we noted that a beam of free electrons in an undulator that provides a sinusoidal magnetic field with wavelength λ_U would produce harmonics q of the device wavelength:

$$\lambda_q \sim \frac{\lambda_U}{2q\gamma^2} \qquad (3)$$

where the electron energy γ is in units of rest mass mc^2. Thus, to vary photon frequency, one can vary γ (or the effective mass m*) or λ_U. For low-energy, conduction-band electrons, $\gamma \sim 1$ so that a wiggle period of $\lambda_U = 60$ μm, achievable with standard IC techniques, might be expected to give 30 μm, 10 THz radiation with angular spread ~1/γ.

III. NOMENCLATURE

In a typical, 2-port, lossy, microwave structure, the power dissipated (normalized to the input power) can be estimated on the assumption that the S-matrix is complex and orthogonal as:

$$P_l = 1 - |S_{11}|^2 - |S_{21}|^2 \geq 0. \qquad (4)$$

The power dissipated can be due to radiation, conductor or substrate loss. For instance, for a standard radiating structure with no output port (S_{21}=0), the dissipated power is dependent on S_{11} only. In this case, small values of S_{11} indicate high loss. Further, we assume that the conductor and substrate losses are much less than radiation loss. This appears to be borne out by measurements on a prototype structure [1] and typical microstrip lines. The radiated power then goes inversely as $|S_{11}|^2$ and one can define the radiation efficiency as the ratio of radiated power to total applied power:

$$\eta = \frac{P_l}{P_t} \qquad (5)$$

IV. TECHNIQUE AND NOMENCLATURE VALIDATION

Finite-Difference, Time-Domain (FDTD) is a powerful and flexible technique that is expected to play a central role in development and simulation of sub-millimeter wave devices. It was chosen here because it is very efficient and its implementation is straightforward. It is ideal for our problem where future research may include anisotropies and non-linearity, and where high pulsed currents are important. Before attempting any simulations, the developed FDTD code required validation. Figure 2 gives sample comparison curves between the FDTD code and HFSS for the radiation efficiency. The results were obtained by simulating a periodic structure such as shown in Fig. 1 with the dimensions given in the caption for Fig. 2. The substrate in Fig.1 is assumed to be duriod with relative permittivity of 2.2. The substrate thickness adjusted for a given width w to give matched, 50 Ω characteristic impedances. In Fig. 2, the radiation efficiency is estimated using two different approaches, i.e. FDTD calculations based on Eqs. (4) and (5) and the integration of the far-field Poynting vector using HFSS. Considering Fig. 2, one also validates the nomenclature provided in Section III.

V. Proposed Technique and Radiation Efficiency Calculations

The proposed technique is based on employing FDTD simulations of one *isolated* cell to obtain its S-parameters. The FDTD domain size was 100 Δx by 32 Δy by 100 Δz. The step sizes Δx, Δy, and Δz were 0.389, 0.265 and 0.4 μm. The time-step (Δt) satisfied the CFL condition. The standard, perfectly matched layer (PML) approach was used to truncate the domain and eliminate any reflections coming back into the computational domain. The structure was excited using a Gaussian pulse with period corresponding to the maximum frequency of interest. The S-parameters for one cell, obtained using the FDTD technique, were converted to an ABCD matrix which was then multiplied *n* times by itself to obtain the entire n-period structure matrix. The resulting ABCD matrix was then converted back to S-parameters [5]. Sample comparison results for this technique with the standard FDTD simulations are shown in Figs. (3)-(5), where good agreement is observed for two and three periods. Finally, the matrix technique was used to calculate radiation efficiency based on Eqs. (4) and (5) for a higher number of cells *n* as shown in Fig. 6. Around 14 THz, the power spectrum becomes narrower and the peak efficiency increases faster than linearly with *n*. Near 18 THz, the 90° bends are both radiating and reflecting more with the fundamental pair radiations for each cell being out of phase from cell-to-cell because d=0.5R emphasizes their higher harmonics. Comparing the n=1 case in Fig. 6 against Fig. 2 clearly shows the coherent addition of field amplitudes.
Thus, the hybrid FDTD technique should be usable in conjunction with any optimization technique to efficiently and easily design periodic structures e.g. to provide coherent interference between radiated fields from successive cells.

VI. Conclusions

We presented electromagnetic simulations of on-chip THz configurations based on a hybrid FDTD technique. The method exploits the characteristics of the ABCD parameters for rapid calculation of S-parameters and radiation efficiency of periodic structures. Results are validated by comparing several calculations from the developed hybrid FDTD code, standard FDTD code, and a commercial, finite-element code (HFSS) that all agreed quite well. Our main goal was to concentrate on the radiative characteristics and determine whether our calculations of the underlying electromagnetics were sound. Other important questions to be pursued on the physical device side are quite fundamental if we want to achieve the predicted operating features such as coherence and tunability. On the production side, the challenges don't lie in the feature sizes but rather in the materials and operating conditions such as the excitation (electronic or optical), proper transport conditions and replenishing the pulse current and voltage as the radiation process proceeds at high efficiency.

Acknowledgement: This work was supported by the US Dept. of Energy contract #*DE-ACO2-76SF00515.*

References

[1] Y. A. Hussein and J. E. Spencer, "Novel possibilities for coherent radiation sources," *in Proc. IEEE MTT-S Int. Sym. Dig.*, 2004, pp.365-368.

[2] P. H. Siegel, "Terahertz technology," *IEEE Trans. Microwave Theory Tech*., vol. 50, No. 3, pp. 910-928, Mar. 2002.

[3] P. H. Siegel, "Terahertz technology in biology and medicine," *IEEE Trans. Microwave Theory Tech*., vol. 52, No. 10, pp. 2438-2447, Oct. 2004.

[4] The Stanford HEPLs FIREFLY undulator typically produces ≤ 1 W of 15-85 μm radiation with a 30 MeV superconducting linac while FELIX in the Netherlands produces 20-250 μm at comparable power.

[5] D. Pozar, *Microwave Engineering.* NJ: John Wiley & Sons, 2005.

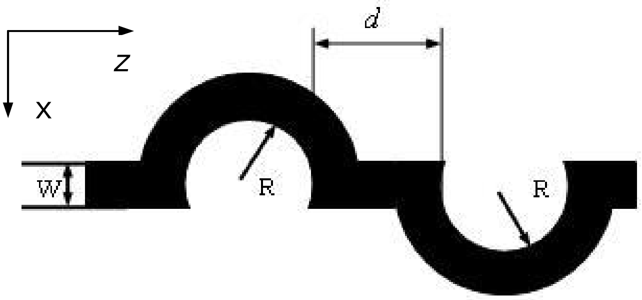

Fig. 1. The metallic top-view of two opposing half-circles (not to scale) separated by a distance *d*. R = 4 μm and W= 2 μm. We note that the HFDTD method is limited to *d* > W. In general, the tuning parameters for optimization are impedance parameters *w/h*, shape parameters e.g. *R*, phase parameter *d*, and material parameter ϵ.

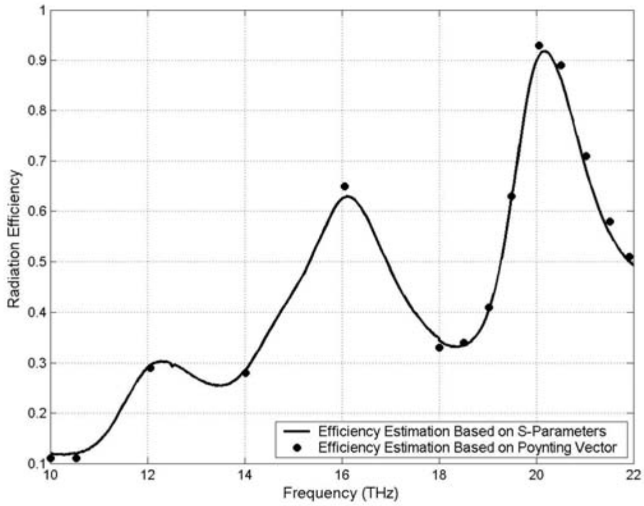

Fig. 2. Radiation efficiency comparisons for a structure such as shown in Fig. 1 when *d*=2.0 and *R*=3.6 µm. Solid line is FDTD, dotted is with HFSS. Also, compare these to the *n*=1 case in Fig. 6.

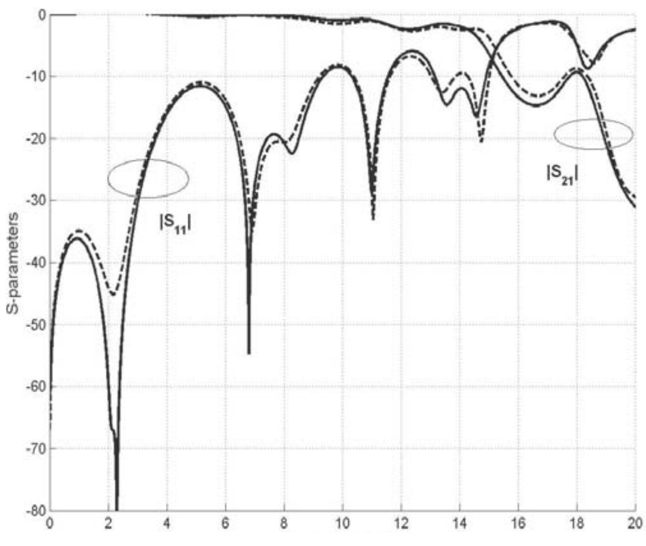

Fig. 3. S-parameters versus frequency (THz) comparison curves (n=2, *d*=2R) obtained by two different approaches. Dashed-line, using FDTD simulation for the entire periodic structure. Solid-line, using the hybrid FDTD technique.

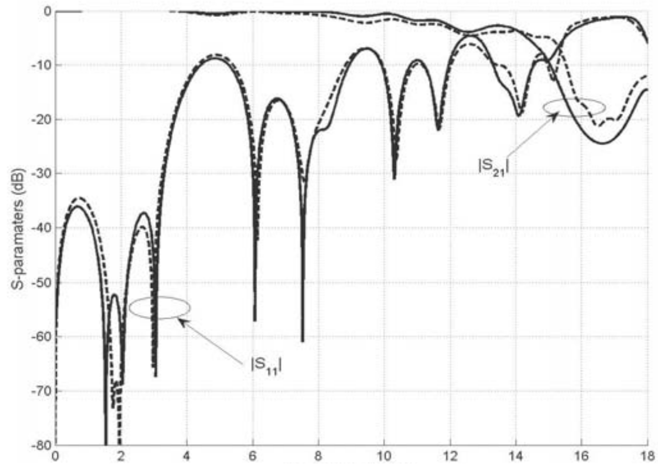

Fig. 4. S-parameters comparison versus frequency (THz) curves (n=3, *d*=2R) obtained by two different approaches. Dashed-line, using FDTD simulation for the entire periodic structure. Solid-line, using the hybrid FDTD technique.

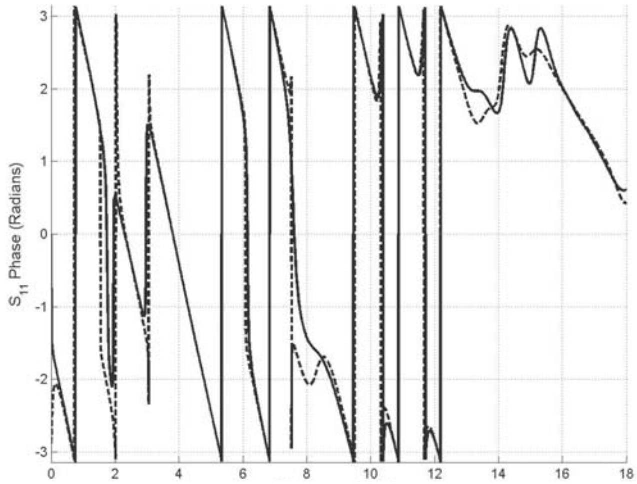

Fig. 5. Return loss phase versus frequency (THz) comparison curves (n=3, *d*=2R) obtained by two different approaches. Dashed-line, using FDTD simulation for the entire periodic structure. Solid-line, using the hybrid FDTD technique.

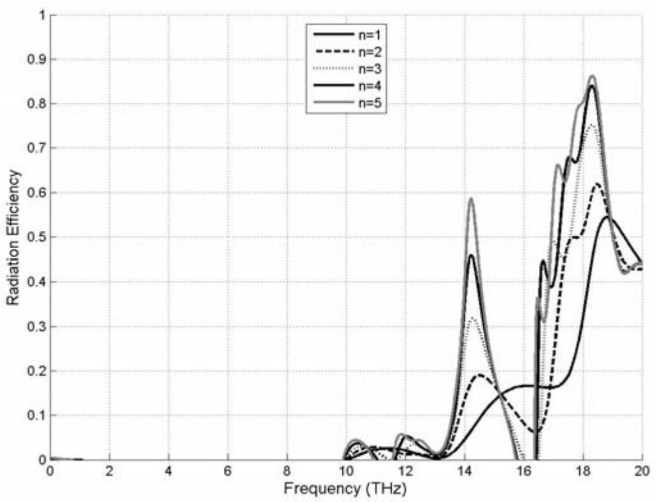

Fig. 6. Radiation efficiency for the structure shown in Fig. 1 when modified with the half-circles facing up and *d*=0.5*R* for different periods using the proposed technique and Eqs. (4)-(5).